Journal of Hydrosciences and Environment
Available online at http://jhe.usb.ac.ir/

ISSN: 2345-5608

# A study of the Homogenous Rainfall Zones of Iran Using Cluster Analysis Based on TRMM Satellite Data

*M. Fatemi[1*], M. Narangifard[2], Kh. Hatami Bahman Beiglou[3]*

*1. Associate Professor of Climatology, Meybod University, Meybod. Iran*
*2. PHD graduate of Climatology , Yazd University, Yazd, Iran*
*3. PHD graduate of Climatology, University of Isfahan, Isfahan, Iran.*

**ARTICLEINFO**

**Article history:**

**Received:** *2 May 2018*
**Accepted:** *26 August 2018*

**Keywords:**
*Precipitation Regions,*
*TRMM,*
*Clustering analysis (CA),*
*Iran.*

**ABSTRACT**

This study aims to evaluate Spatio-temporal distribution of rainfall through cluster analysis based on Tropical Rainfall Measuring Mission (TRMM) in Iran. To this purpose, the daily-gridded rainfall data were derived for the 1998-2013 period. Then, the seasonal and annual time scale cluster analysis was performed on TRMM-derived rainfall data. The results identified 14 clusters in the annual rainfall. As a high- rainfall zone, Guilan has an average rainfall of 1068 mm per year while Sistan, as a low-rainfall area, has an average rainfall of 106.8 mm annually. Furthermore, the seasonal rainfall distribution indicates high-rainfall zones in Guilan and Mazandaran provinces in spring, summer, and autumn while the areas in the southern range of Alborz Mountain and Persian Gulf are clustered as low-rainfall zone. The rainfall distribution in Iran is seasonal, and the following provinces are among the high-rainfall zones in winter: Kohgiluyeh and Boyer Ahmad, Chaharmahal and Bakhtiari, Khuzestan, and highlands of Lorestan. The low-rainfall areas also include Sistan and Baluchistan, Yazd, and Semnan.

## 1. Introduction

As a fundamental component of the global water cycle, precipitation is a key parameter in ecology, hydrology and meteorology. It plays an important role in energy exchange and material circulation in the surface system of the Earth. Therefore, it is of significant importance to understand the spatial and temporal variation characteristics of precipitation. Traditional precipitation data are usually derived from point measurements, which rely heavily on field observations (Jia et al., 2011: 3069). Accurate rainfall data is essential for numerous applications (Mantas et al., 2014: 1) including hydrologic modeling, disaster monitoring and preparedness activities. However, it is difficult to obtain observational precipitation data, especially in remote areas, continents and oceans, where gauge and radar networks are sparse (Liu, 2015: 119). In developing countries, particularly in arid countries, there is a paucity of continuous rain gauge precipitation measurements to undertake time series analyses (Ud din et al., 2008: 1320). An estimation of precipitation solely based on gauge networks is not desirable (Huang et al., 2014: 410). Many attempts have been made to develop and improve global and regional gridded precipitation gauge data sets in recent years (Javanmard et al., 2010: 119). The observation of rainfall rate by rain gauges is only based on point measurements, lacking spatial representativeness, particularly during convective events of small spatial sizes (Chwala et al., 2014: 57). The remote sensing of precipitation, especially rainfall, by the satellite-borne remote sensor is of paramount importance (Okamoto et al., 1979: 1043). Satellite remote sensing techniques play a pivotal role in filling data gaps (Liu, 2015: 119).

Satellite-based rainfall remote sensing has been an active research field for over three decades (Liu and Fu, 2010: 436). A number of studies have applied TRMM satellite data to various regions such as in the Middle East and Mediterranean (Ud din et al., 2008; Javanmard et al., 2010; Almazroui, 2011; Ahmadi and Narangifard, 2012; Moazami et al., 2013; Nastos et al., 2013; Mozafari and Narangifard, 2016; Darand et al., 2017; Kiany et al., 2018), India (Mishra et al., 2012), Bangladesh (Moffitt et al., 2011), China (Jia et al, 2011; Li et al., 2012; Du et al., 2013, Zhang et al., 2018; Li et al., 2018), South Africa (Olurotimi et al., 2017), Iberian Peninsula (Immerzeel et al., 2009), peninsular Malaysia (Varikoden et al., 2010) and Palestine West Bank (Khalaf and Donoghue, 2012).

This study aims to perform a cluster analysis of rainfalls in Iran using TRMM satellite data.

* Corresponding author's email: *yazdfatemi@yahoo.com*

## 2. Dataset and Methodology

### 2.1. Study area

Comprising a land area of around 1648000 square kilometer, Iran is located in the Middle East. It lies between latitudes 24° and 40° N, and longitudes 44° and 64° E. The two major high mountain ranges of Iran, Zagros across the western boundary and Alborz in the north, influence the Spatio-temporal patterns of precipitation, preventing much of the moisture from spreading to the interior deserts (Darand and Daneshvar, 2014: 518). This dataset covers the area between 20° E - 65° E and 15° N - 4 5° N, with a resolution of 0.25°×0.25°, which is clipped in 2484 pixels over Iran (Fig. 1).

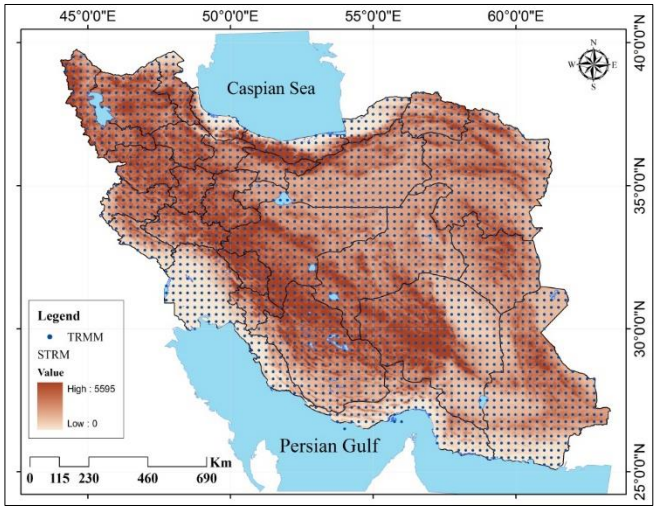


**Figure 1.** The clipped TRMM dataset on the elevation map of Iran containing 2484 grids with a resolution of 0.25°×0.25°

### 2.2. Data sources

TRMM was launched in November 1997, but the onboard precipitation radar was adjusted to the observation mode in December 1997 (Gabella et al., 2011: 2). After about a decade of operation, the TRMM satellite has provided researchers with a large volume of rainfall data for the assessment of atmospheric and climate models. Given operational challenges over the oceans, it is difficult to measure rainfall with rain gauges and hence remotely sensed data of rainfall serves as the only source of reliable and continuous data (Shrivastava et al., 2014: 132). TRMM 3B42 generally provides a smoother precipitation field than that of gauge data due to the temperature structure of clouds. In areas of high gauge density, TRMM 3B42 has a comparatively coarser spatial resolution. A relatively real-time estimate of precipitation from satellite measurements is accessible with a 9-hour time lag at a 3-hourly interval. Additional estimates calibrated with ground measurements are subsequently within 10e15 days from the end of the month (Duncan and Biggs, 2012: 628).

TRMM dataset 3B43 V6 (between 50° south and 50° north) is often used to estimate rainfall. Its products (TRMM data) have become a reference standard in comparison with all other satellite-derived products. The dataset employed in this study is TRMM 3B43 (http://disc2.nascom.nasa.gov). These gridded estimates have a calendar-month temporal resolution and a spatial resolution of 0.25°×0.25°. Since this study is concerned with the downscaling algorithm for annual precipitation, the annual precipitation from 1998 to 2013 was calculated by accumulating monthly TRMM 3B43 data for twelve months of a year.

## 3. Cluster analysis

Clustering algorithms group datasets based on homogeneity. They usually employ a distance measure to quantify the degree of correspondence of events and utilize a linkage algorithm to allocate an event to a particular cluster (Erfani and Chouinard, 2012: 62). In other words, cluster analysis aggregates observations into clusters so that each observation is as homogeneous as possible with respect to the clustering variables (Izquierdo et al., 2014: 484).

Ward's linkage uses the incremental sum of squares, i.e. the increase in the total within-cluster sum of squares caused by joining two clusters. The within-cluster sum of squares is defined as the sum of squares of distances between all objects in the cluster and the centroid of the cluster. The sum of squares measure is equivalent to the following distance measure d(r,s), which constitutes the formula used in linkage:

$$d(r,s) = \sqrt{\frac{2n_r n_s}{(n_r+n_s)}} ||x_r - x_s||2' \qquad (1)$$

Where $\| \|_2$ is Euclidian distance $X_r$, $X_s$ are centroids of clusters $r$ and $s$, $n_r, n_s$ are the number of elements in clusters $r$ and $s$. In some references, factor 2 is not used in Ward's linkage to multiply nrns. The linkage function utilizes this factor so that the distance between two singleton clusters remains equal to the Euclidean distance (Kaufman and Rousseeuw, 2009). To calculate integration or data binding, the Ward's method was used:

$$d(C_i \cup C_j, C_k) = \frac{n_i+n_k}{n_i+n_j+n_k} d(C_i, C_k) + \frac{n_i+n_k}{n_i+n_j+n_k} d(C_i, C_k) - \frac{n_i+n_k}{n_i+n_j+n_k} d(C_i, C_j) \qquad (2)$$

Where d is the Euclidean distance of cluster and I, j, k (C= Cluster) - $C_i$, $C_j$, $C_K$ constitute a separate cluster.

## 4. Results and Discussions

### 4.1. Interpretation of cluster analysis

The annual precipitation data, annual rainfall zones, and the rainfall zones of Iran were classified into 12 clusters (Fig. 2) as follows:

The cluster rainfall zone of Sistan covers 14.4% of Iranian land area. It embraces the provinces of Sistan and Baluchestan in the southeast of Iran as well as the east of Kerman and Hormozgan provinces. The average annual rainfall in this zone is 106.8 mm. Kerman - Hormozgan zone covers 13.2% of the land area of Iran. The average annual rainfall in this zone is 127.8 mm. In the cluster of Fars- Bushehr zone, the total annual rainfall is 270 mm and it constitutes 5.1% of the total land area of Iran. Kohgiloyeh and Boyer Ahmad zone covers 6.1% of Iranian area with an average annual rainfall of 534 mm. In the central - eastern zone, the total annual rainfall is 136.8 mm and it constitutes 28.7% the total area of Iran. Ilam- Kermanshah zone covers 4.4% of the area of Iran with an average annual rainfall of 486 mm. In Hamadan -West Azerbaijan zone, the total annual rainfall is 342 mm and it covers 7.5% of the total area of Iran. Khorasan- Central zone accounts for 10.8% of Iranian area with an average annual rainfall of 273.6 mm. In Ardabil- Alborz zone, the total annual rainfall is 511.2 mm and it constitutes 4% of the total area of Iran. The total annual rainfall in Mazandaran zone is 763.2 mm and it accounts for 1.4% of the total area of Iran. East Azerbaijan zone covers 3.6% of the land area of Iran with an average annual rainfall of 360 mm. The total annual rainfall in Gilan zone is 1068 mm and it accounts for 0.6% of the total area of Iran.

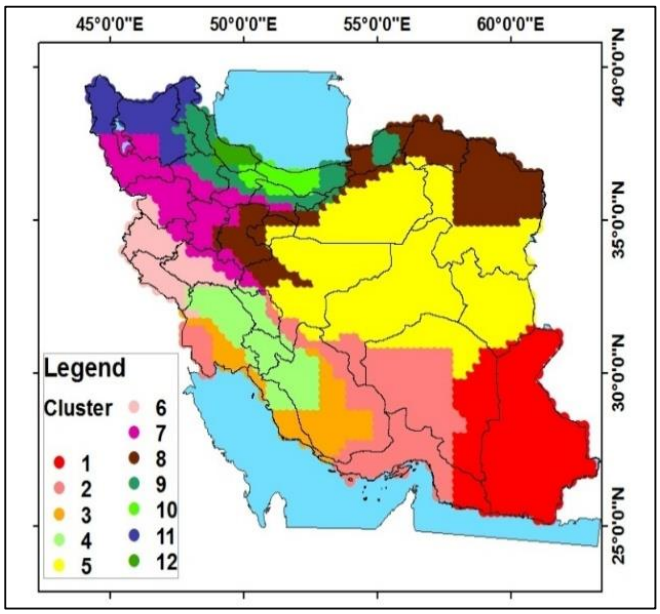


**Figure 2.** Annual rainfall clustering in Iran

Discussion of cluster analysis of the seasonal precipitation data

### 4.2. Precipitation clustering in spring

In the zones under study, rainy springs were classified into four clusters (Fig. 3) as follows:

A *very low rainfall* zone with a land area of 926834 km, which constitutes 56.24% of the total area of Iran, this zone represents areas with an average rainfall of 17 mm. A *low rainfall* zone accounts for 23.03% (379491 km) of the land area of Iran with an average annual rainfall of 33 mm. A *high rainfall* zone with an area of 209322 km that constitutes 12.64% of the total land area of Iran, and represents areas with an average rainfall of 42 mm. A *very high rainfall* that accounts for 8.09% (133352 km) of Iranian area, with an average annual rainfall of 51 mm.

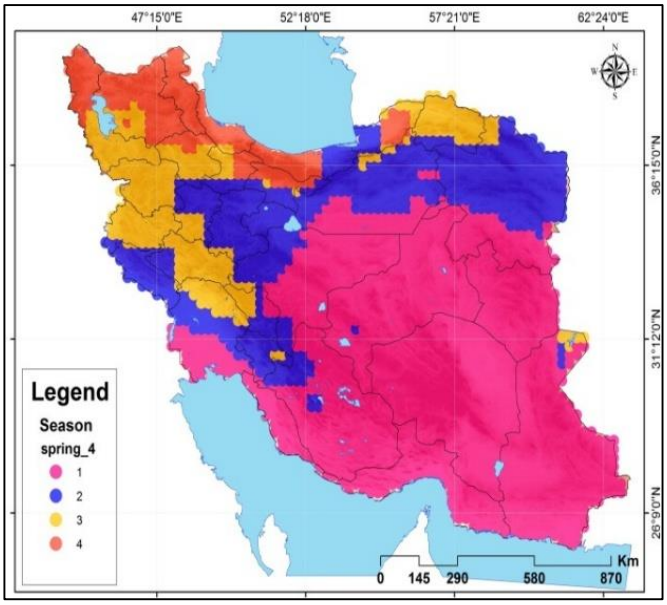


**Figure 3:** Spring rainfall clustering in Iran

### 4.3. Precipitation clustering in summer

In the zone under study, rainy summers were classified into five clusters (Fig. 4) as follows:

A *very low rainfall* zone that constitutes 85.51% (1409159 km) of the total area of Iran and represents areas with an average rainfall of 5.5 mm. A *low rainfall zone* with an area of 129372 km (7.85% of the total area of Iran) which covers areas with an average rainfall of 7.6 mm. A *semi-rainfall zone* accounting for 4.39% (72315 km) of the area of Iran with an average annual rainfall of 9.6 mm. A high rainfall zone with an area of 27201 km – (1.65% of the total area of Iran), which represents areas with an average rainfall of 10.7 mm. A very high rainfall zone with an area of 9951 km (0.6% of the total area of Iran), which covers areas with an average rainfall of 11.5 mm.

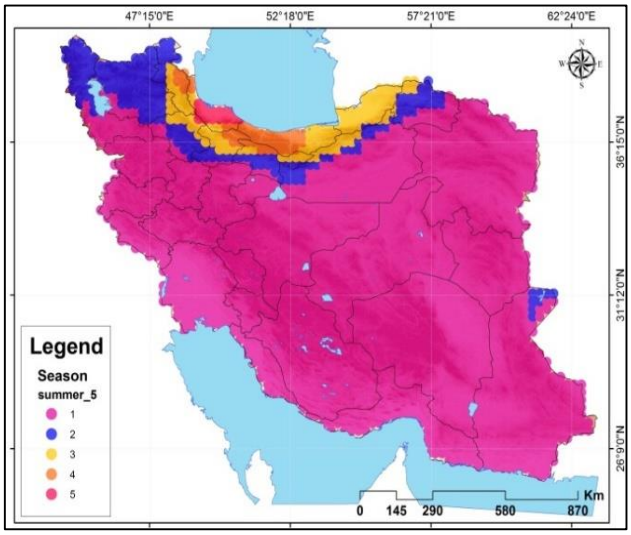


**Figure 4:** Summer rainfall clustering in Iran

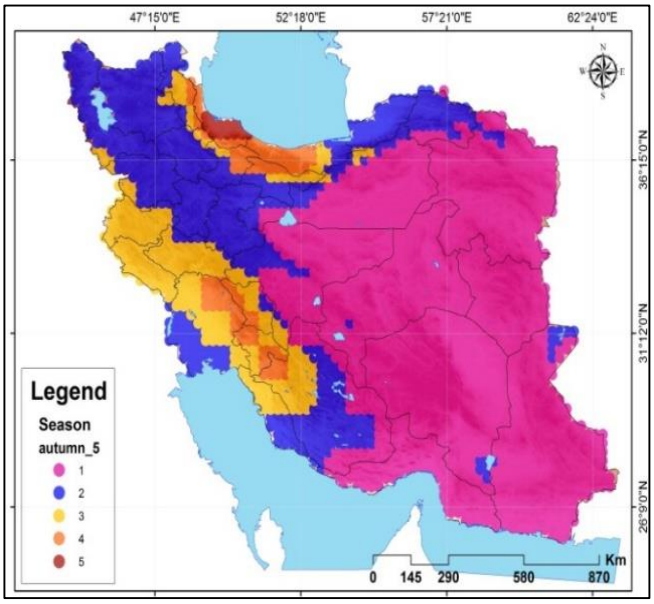


**Figure 5:** Autumn Annual rainfall clustering in Iran

### 4.4. Precipitation clustering in autumn

In the zones under study, the rainy autumn was classified into five clusters (Fig. 5) as follows:

A *very low rainfall* zone with an area of 979246 km (59.43% of the total area of Iran), which covers areas with an average rainfall of 32 mm. A *low rainfall* zone with an area of 404038 km (24.52% of the total area of Iran), which represents areas with an average rainfall of 58 mm. A *semi-rainfall* zone with an area of 187755 km (11.39% of the total area of Iran), which covers areas with an average rainfall of 72 mm. A high rainfall zone with an area of 67671 km (4.11% of the total area of Iran) which represents areas with an average rainfall of 78 mm. A *very high rainfall* zone with an area of 9288 km (0.56% of the total area of Iran), which covers areas with an average rainfall of 80 mm.

### 4.5. Precipitation clustering in winter

In the zones under study, the rainy winter was classified into five clusters based (Fig. 6) as follows:

A *very low rainfall* zone that constitutes 33.01% (544025 km) of the total land area of Iran, representing areas with an average rainfall of 63 mm. A *low rainfall* zone with an area of 555967 km (33.74% of the total area of Iran), which covers areas with an average rainfall of 101 mm. A *semi-rainfall* zone with an area of 72979 km, (4.43% of the total area of Iran), which represents areas with an average rainfall of 114 mm. A *high rainfall* zone that constitutes 16.3% (268695 km) of the total area of Iran, representing areas with an average rainfall of 124 mm. A high rainfall zone with an area of 139323 km (8.45% of the total area of Iran), which covers areas with an average rainfall of 147 mm. A *very high* rainfall zone with an area of 67008 km (4.07% of the total area of Iran), which represents areas with an average rainfall of 160 mm.

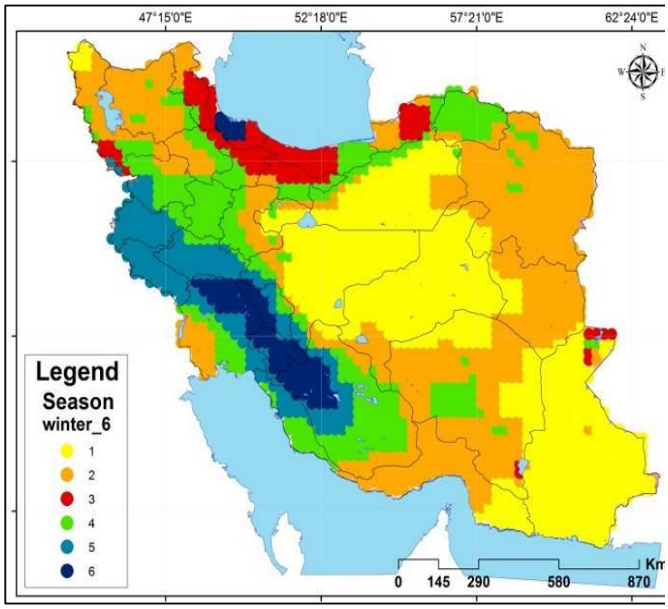


**Figure 6:** Winter rainfall clustering in Iran

## 5. Conclusions

In this study, using TRMM satellite data, the precipitation clusters were identified in the 1998-2013 period based on annual rainfall and seasons. According to the time scale of the territory's annual rainy zones, Gilan and Mazandaran province with an average rainfall of 763.2 mm and 1068 mm had the highest rainfall, respectively, and Sistan province with an average rainfall of 106.8 mm had the lowest rainfall. The most extensive rainfall zone was the central - eastern region (accounting for 28.7% of the total area of Iran) with an average precipitation of 136.8 mm. According to the seasonal time scale, rainy springs were classified into four clusters. A very low rainfall zone constituting 56.24% of the total area of Iran, which covers areas with an average rainfall of 17 mm. A low rainfall zone accounting for 23.03% of the area of Iran, with an average annual rainfall of 33 mm. A high rainfall zone constituting 12.64% of the total area of Iran, which represents areas with an average rainfall of 42 mm. A very high rainfall zone accounting for 8.09% of the total area of Iran, with an average annual rainfall of 51 mm. In addition, rainy summers were classified into five clusters. A very low rainfall zone accounting for 85.51% of the total area of Iran with an average annual rainfall of 5.5 mm. A low rainfall zone constituting 7.85% of the area of Iran with an average rainfall of 7.6 mm. A semi-rainfall zone accounting for 4.39% of the total area of Iran, with an average rainfall of 9.6 mm. A high rainfall zone that accounts for 1.65% of the total area of Iran, with an average annual rainfall of 10.7 mm. A very high rainfall zone that constitutes 0.6% of the total area of Iran with an average rainfall of 11.5 mm. Moreover, rainy autumn was also classified into five clusters. A very low rainfall that accounts for 59.43% of the total area of Iran with an average annual rainfall of 32 mm. A low rainfall zone that accounts for 24.52% of Iran with an average rainfall of 58 mm. A semi-rainfall zone that constitutes 11.39% of the total area of Iran with an average rainfall of 72 mm. A high rainfall zone that accounts for 4.11% of the total area of Iran with an average annual rainfall of 78 mm. A very high rainfall zone that constitutes 0.56% of the total area of Iran with an average rainfall of 80 mm. In the same vein, the rainy winter was classified into five clusters. A very low rainfall zone that accounts for 33.01% of the total area of Iran with an average rainfall of 63 mm. A low rainfall zone that constitutes 33.74% of the total area of Iran with an average rainfall of 101 mm. A semi-rainfall zone that covers 4.43% of the total area of Iran with an average rainfall of 114 mm. A high rainfall zone that constitutes 16.3% of the total area of Iran with an average rainfall of 124 mm. A very high rainfall zone that covers 8.45% of the total area of Iran with an average rainfall of 147 mm. A very high rainfall zone that constitutes 4.07% of the total area of Iran with an average rainfall of 160 mm. The provinces of Gilan, Mazandaran and the southern slopes of the Alborz Mountains had the lowest rainfall in spring, summer and autumn. In winter, the precipitation rate was different from other seasons with the highest rainfall being recorded in Kohgiluyeh and Boyer Ahmad, Chahar Mahal Bakhtiari and Khuzestan and Lorestan provinces and the lowest rainfall in the provinces of Sistan and Baluchistan, Isfahan, Yazd and Semnan. The findings suggested that TRMM satellite data could be used to study and identify clusters of rainfall, especially in areas with few ground stations.

## 6. References

1. Ahmadi M., Narangifard M., 2012. Assessment precipitation regions in Fars province using TRMM satellite data. Researches in Earth Sciences; 3(11), PP 28-44.
2. Almazroui M., 2011. Calibration of TRMM rainfall climatology over Saudi Arabia during 1998–2009. Atmospheric Research; 99(3), PP 400-414.
3. Chwala C., Kunstmann H., Hipp S., & Siart, U. 2014. A monostatic microwave transmission experiment for line integrated precipitation and humidity remote sensing. Atmospheric Research; 144, PP 57-72.
4. Darand M., Daneshvar M. R. M., 2014. Regionalization of Precipitation Regimes in Iran Using Principal Component Analysis and Hierarchical Clustering Analysis. Environmental Processes; 1(4), PP 517-532.
5. Darand, M., Amanollahi, J., & Zandkarimi, S. (2017). Evaluation of the performance of TRMM Multi-satellite Precipitation Analysis (TMPA) estimation over Iran. Atmospheric Research, 190, 121-127.
6. Du, L., Tian, Q., Yu, T., Meng, Q., Jancso, T., Udvardy, P., & Huang, Y. (2013). A comprehensive drought monitoring method integrating MODIS and TRMM data. International Journal of Applied Earth Observation and Geoinformation, 23, 245-253.

7. Duncan J. M., Biggs E. M., 2012. Assessing the accuracy and applied use of satellite-derived precipitation estimates over Nepal. Applied Geography; 34, PP 626-638.

8. Erfani R., Chouinard L. 2012. Automated synoptic typing of freezing rain events for hazard analysis. Atmospheric Research; 111, PP 58-70.

9. Gabella M., Morin E., Notarpietro R., Michaelides S., 2011. Winter precipitation fields in the Southeastern Mediterranean area as seen by the Ku-band space borne weather radar and two C-band ground-based radars. Atmospheric Research; 119, PP 120-130.

10. http://disc2.nascom.nasa.gov

11. Huang C., Zheng X., Tait A., Dai Y., Yang C., Chen, Z. ... & Wang, Z. 2014. On using smoothing spline and residual correction to fuse rain gauge observations and remote sensing data. Journal of Hydrology; 508, PP 410-417.

12. Immerzeel W. W., Rutten M. M., & Droogers P. 2009. Spatial downscaling of TRMM precipitation using vegetative response on the Iberian Peninsula. Remote Sensing of Environment; 113(2), PP 362-370.

13. Izquierdo R., Alarcón M., Aguillaume L., Àvila A. 2014. Effects of teleconnection patterns on the atmospheric routes, precipitation and deposition amounts in the north-eastern Iberian Peninsula. Atmospheric Environment; 89, PP 482-490.

14. Javanmard, S., Yatagai, A., Nodzu, M. I., BodaghJamali, J., & Kawamoto, H. (2010). Comparing high-resolution gridded precipitation data with satellite rainfall estimates of TRMM_3B42 over Iran. Advances in Geosciences, 25, 119-125.

15. Jia S., Zhu W., Lű A., Yan T., 2011. A statistical spatial downscaling algorithm of TRMM precipitation based on NDVI and DEM in the Qaidam Basin of China. Remote sensing of Environment; 115(12), PP 3069-3079.

16. Kaufman L., Rousseeuw P. J., 2009. Finding groups in data: an introduction to cluster analysis John Wiley & Sons; Vol. 344.

17. Khalaf A., Donoghue D., 2012. Estimating recharge distribution using remote sensing: A case study from the West Bank. Journal of Hydrology; 414, PP 354-363.

18. Kiany, M. S. K., Balling Jr, R. C., Cerveny, R. S., & Krahenbuhl, D. S. (2018). Diurnal variations in seasonal precipitation in Iran from TRMM measurements. Advances in Space Research. 9(62), 2418-2430.

19. Li X. H., Zhang Q., Xu C. Y., 2012. Suitability of the TRMM satellite rainfalls in driving a distributed hydrological model for water balance computations in Xinjiang catchment, Poyang lake basin. Journal of Hydrology; 426, PP 28-38.

20. Li, D., Christakos, G., Ding, X., & Wu, J. (2018). Adequacy of TRMM satellite rainfall data in driving the SWAT modeling of Tiaoxi catchment (Taihu lake basin, China). Journal of Hydrology, 556, 1139-1152.

21. Liu Q., Fu Y. 2010. Comparison of radiative signals between precipitating and non-precipitating clouds in frontal and typhoon domains over East Asia. Atmospheric Research; 96 (2), PP 436-446.

22. Liu Z., 2015. Comparison of precipitation estimates between Version 7 3-hourly TRMM Multi-Satellite Precipitation Analysis (TMPA) near-real-time and research products. Atmospheric Research; 153, PP 119-133.

23. Mantas V. M., Liu Z., Caro C., Pereira A. J. S. C., 2014. Validation of TRMM multi-satellite precipitation analysis (TMPA) products in the Peruvian Andes. Atmospheric Research.

24. Mishra A. K., Gairola R. M., Agarwal V. K. 2012. Rainfall Estimation from Combined Observations Using KALPANA-IR and TRMM-Precipitation Radar Measurements over Indian Region. Journal of the Indian Society of Remote Sensing; 40(1), PP 65-74.

25. Moazami, S., Golian, S., Kavianpour, M. R., & Hong, Y. (2013). Comparison of PERSIANN and V7 TRMM Multi-satellite Precipitation Analysis (TMPA) products with rain gauge data over Iran. International Journal of Remote Sensing, 34(22), 8156-8171.

26. Moffitt C. B., Hossain F., Adler R. F., Yilmaz K. K., Pierce H. F., 2011. Validation of a TRMM-based global Flood Detection System in Bangladesh. International Journal of Applied Earth Observation and Geoinformation; 13(2), PP 165-177.

27. Mozafari G. A., Narangifard M. 2015. The Vegetative Cover Deterioration Due to the Droughts on the Mulla Sadra Watershed and Application of Remote Sensing Techniques in Its Monitoring. Water Engineering; 8(26), PP 1-14.

28. Nastos, P. T., Kapsomenakis, J., & Douvis, K. C. (2013). Analysis of precipitation extremes based on satellite and high-resolution gridded data set over Mediterranean basin. Atmospheric Research, 131, 46-59.

29. Okamoto K., Miyazaki S., Ishida T. 1979. Remote sensing of precipitation by a satellite-borne microwave remote sensor. Acta Astronautica; 6(9), PP 1043-1060.

30. Olurotimi, E. O., Sokoya, O., Ojo, J. S., & Owolawi, P. A. (2017). Observation of bright-band height data from TRMM-PR for satellite communication in South Africa. Journal of Atmospheric and Solar-Terrestrial Physics, 160, 24-33.

31. Shrivastava R., Dash S.K. Hegde M.N. Pradeepkumar K.S. Sharma D.N. 2014, Validation of the TRMM Multi Satellite Rainfall Product 3B42 and estimation of

scavenging coefficients for 131I and 137Cs using TRMM 3B42 rainfall data, Journal of Environmental Radioactivity; 138, PP 132-136.

32. Ud din S., Al-Dousari A., Ramdan A., Al Ghadban A. 2008. Site-specific precipitation estimate from TRMM data using bilinear weighted interpolation technique: An example from Kuwait. Journal of arid environments; 72(7), PP 1320-1328.

33. Varikoden H., Samah A. A., Babu C. A. 2010. Spatial and temporal characteristics of rain intensity in the peninsular Malaysia using TRMM rain rate. Journal of hydrology; 387(3), PP 312-319.

34. Zhang, T., Li, B., Yuan, Y., Gao, X., Sun, Q., Xu, L., & Jiang, Y. (2018). Spatial downscaling of TRMM precipitation data considering the impacts of macro-geographical factors and local elevation in the Three-River Headwaters Region. Remote Sensing of Environment, 215, 109-127.